Design of a Wrist-Worn Device for Simultaneous Detection of ECG and Cardiac Pulse: A Preliminary Study

Rafael Gonzalez-Landaeta[1](✉), Aldo Rodrigo Mejía Rodríguez[2], Guadalupe Dorantes Mendez[2], and Dora-Luz Flores[3]

[1] BIOCIM Research Group, Universidad Autónoma de Ciudad Juárez, Ciudad Juárez, Chihuahua 32310, México
rafael.gonzalez@uacj.mx

[2] Faculty of Sciences, Universidad Autónoma de San Luis Potosi, 78295 San Luis Potosi, México

[3] Facultad de Ingeniería, Universidad Autónoma de Baja California, Arquitectura y Diseño, Ensenada, Baja California 22860, México

Abstract. Wearable systems, such as watch/wristband systems must deal with power consumption and power line interference problems without compromising the form factor of the device and the signal-to-noise ratio (SNR). In this study, we present a preliminary design of a wrist-worn device that simultaneously detects ECG and cardiac pulse. Unlike the systems currently available in the market, the cardiac pulse is measured by detecting the magnetic disturbance caused by the blood flow in a localized magnetic field, eliminating the need to use optical sensors, which demand higher currents. The device's circuitry was implemented using surface mount technology (SMT) on a 43.5 x 32.5 mm 4-layer PCB. With these dimensions, the contribution of electromagnetic interferences was lower than 42.5 μV when the device was used in an office setting. The main current consumption was lower than 500 μA, and the SNR was higher than 68 dB for the ECG and higher than 55 dB for the pulse signal, enabling a clear identification of the different waves of the detected signals. The aim is to simplify the signal processing algorithms in such a way that several features of the detected signals can be easily identified using fewer hardware resources.

Keywords: ECG · Cardiac Pulse · Wrist-Worn device

1 Introduction

Monitoring of physiological variables in non-hospital settings has become common today. This practice reduces costs in health systems and allows information on the subject's health status to be obtained during their daily activities. Wearable technology has become popular among consumers [1] since there are systems that provide information on heart rate, breathing, mental health, and physical activity, among others [2, 3].

J. de J. A. Flores Cuautle et al. (Eds.): CNIB 2023, IFMBE Proceedings 96, pp. 357–364, 2024.
https://doi.org/10.1007/978-3-031-46933-6_37

The most common wearable systems are smartwatches or bracelet-type devices since they can be worn comfortably for long periods. The most popular are the Apple Watch (Apple), Galaxy Watch (Samsung), ScanWatch (Withings), Sense (Fitbit) [4], and the WHOOP band (WHOOP Inc.) [5]; most of these systems detect various physiological signals, from which they indirectly estimate other parameters, such as blood pressure, blood oxygenation, respiration, stress, and sleep disorders, to name a few. Among the signals that are most detected with these systems are the electrocardiogram (ECG) and the photoplethysmogram (PPG). Regarding the ECG, detection is usually done using two dry electrodes, allowing the detection of a single ECG lead (usually lead-I) [6]. However, in the case of the Apple Watch, studies have been carried out where the primary function of such a device has been extended to measure multiple leads (not simultaneously) [7]. Optical sensors (LEDs and a photodiode) are often used to detect PPG. These sensors are in contact with the skin, making it possible to detect changes in blood volume in peripheral arteries.

ECG sensing using two dry electrodes fits very well into the wearable paradigm. However, it is challenging from the electronic design point of view since the contribution of power line interference (60 Hz), V_{EMI}, depends on the imbalance of the impedances of the electrodes (ΔZ_{E}), the common mode impedance (Z_{C}) of the front end, the common-mode rejection ratio (CMRR) of the system, and the isolation impedance (Z_{ISO}) [8], that is:

$$V_{\mathrm{EMI}} = i_{\mathrm{p}} \frac{Z_{\mathrm{B}}}{Z_{\mathrm{C}} + 2(Z_{\mathrm{B}} + Z_{\mathrm{ISO}})} \left(\Delta Z_{\mathrm{E}} + \frac{Z_{\mathrm{C}}}{CMRR} \right) \tag{1}$$

where i_{p} is the power line displacement current flowing through the body, and Z_{B} is the patient-ground impedance.

Regarding the detection of PPG, the use of LEDs implies a high-power consumption (tens of mW) [9], which considerably reduces the autonomy of the system. However, there are strategies to reduce the consumption of LEDs, the best known is to use a switched-mode power supply [10], but it requires a greater number of electronic components that make electronics bulky.

In this work, a preliminary study is presented focused on the design of a watch/bracelet-type device capable of simultaneously detecting the ECG and the cardiac pulse signal. The aim is to design a low-power electronic circuitry capable to detect two biosignals with high SNR and with a remarkable immunity to power line interferences. To achieve this, a printed circuit board (PCB) was designed to guarantee the signals' integrity. For the ECG detection circuit, those aspects of the electronic design that allow reducing the contribution of line interference and the loading effect with the electrode-skin impedance were also addressed, such as a system with high differential input impedance (Z_{D}), and Z_{C}, a high CMRR, and a high Z_{ISO}. Strategies to reduce electronic noise in the system and maintain low current consumption were also discussed. The method proposed by Phua et al. [11] will be implemented to detect the cardiac pulse. This method detects the disturbance caused by blood on a localized magnetic field. To achieve this, a permanent magnet and a magnetic sensor were placed over a (large-size) artery. This technique requires simple circuits which leads to a lower consumption. This proposal was already presented by Méndez-Lira et al. [12], where it was possible to simultaneously detect the ECG and the cardiac pulse. However, the system consumed

over 10 mA and was developed at the breadboard level, which is far from the ideal design and implementation considerations for a wearable system. The main goal of the proposed system is to track and assess in the future the cardiovascular health, including the automatic detection of the long QT syndrome.

2 Materials and Methods

2.1 ECG Detection Circuit

Figure 1 shows the circuit used for detecting the ECG by two dry electrodes. The front end relied on a fully differential ac-coupling network to achieve a high CMRR and to eliminate the half-cell potential from the electrodes. The input impedance behaves as an inductor, so a high input impedance is ensured at the power line frequency without using very high-value resistors [13]. This reduces the loading effect between the front end and the contact impedance of the dry electrodes, which, according to previous tests, is about 80 kΩ for our custom-built electrodes. The front end has a unity gain, so the instrumentation amplifier (IA) fixed the overall gain. This means that the high gain of the IA amplifies the voltage noise of the front end. To reduce the output noise of the circuit, the noise voltage of the front end must be low. The operational amplifier (OpAmp) used was the LMP2234, a quad micropower amplifier (Texas Instruments) with a noise voltage of 60 nV/$\sqrt{}$Hz @ 1 kHz and current consumption of 34 μA. The IA was the INA826 (Texas Instruments), a rail-to-rail amplifier with a CMRR = 104 dB, a noise voltage of 18 nV/$\sqrt{}$Hz @ 1 kHz, and a current consumption of 200 μA. The ECG circuit was tested in two scenarios: 1) using a TechPatient CARDIO V4 patient simulator (HE Instruments LLC, FL, USA), configured to generate an ECG signal of 1 mV amplitude at 72 bpm. 2) Measuring the lead-I ECG of a volunteer.

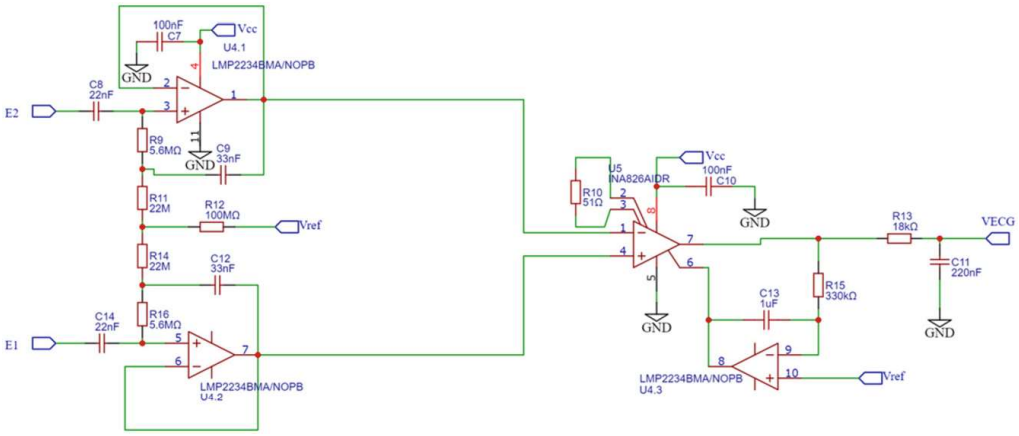

Fig. 1. Electronic circuit for detecting de ECG using two dry electrodes.

2.2 Cardiac Pulse Detection

Magnetic Field Source

The detection of the cardiac pulse is based on the measurement of the disturbance caused by the blood flow on a focused magnetic field. To generate this field, a circular (Diameter = 15 mm) neodymium magnet of 130 mT was used and placed over the radial artery.

Sensor

A TMR2001 (Multi Dimension) tunnel-type magnetoresistive sensor was used to measure the magnetic disturbance. It is a full Wheatstone bridge with a sensitivity of 80 mV/V/mT, an output impedance of 63 kΩ , and consumes 16 uA. To detect the magnetic disturbance, the sensor was placed over the radial artery at a distance of 5 mm from the magnet.

Electronic Circuit

Figure 2 shows the circuit used to detect the cardiac pulse. The differential output of the TMR2001 sensor is connected to the input of this circuit. The front end consists of an IA coupled in ac by a symmetric network that guarantees a high CMRR [14]. With this configuration, zero errors from the sensor in the presence of the constant magnetic field of the magnet are eliminated. The input impedance of this system is 1 MΩ, which reduces loading errors when connected to the magnetic sensor. The IA is the AD627 (Analog Devices, MA, USA); it has a current consumption of 60 μA and a noise voltage of 38 nV/$\sqrt{}$Hz. This circuit was also tested on the same volunteer.

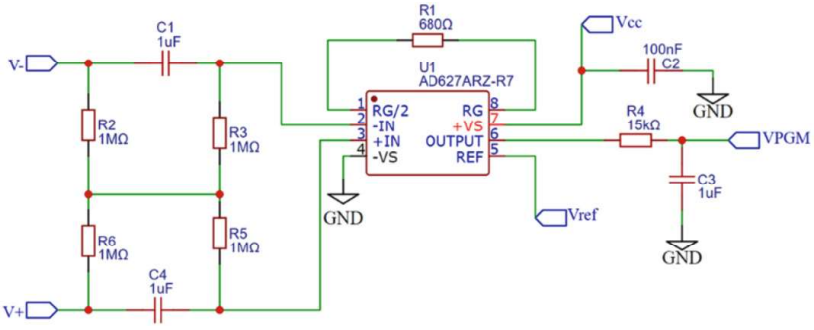

Fig. 2. Electronic circuit for detecting de cardiac pulse.

2.3 Printed Circuit Board Design

All electronic circuits were implemented using surface mount technology (SMT). In addition to the circuits in Figs. 1 and 2, a battery charging circuit that uses a Micro-B SMD USB connector, a 3.3 V voltage regulator circuit, and a 1.65 V reference voltage were also included. Although we are working with low-frequency signals, the PCB design seeks to guarantee the integrity of the signal for the subsequent integration of digital circuits and wireless transmission systems. For this, a 4-layer PCB was designed

with dimensions of 43.5 mm × 32.5 mm. The top layer (Fig. 3a) contains all the circuitry. The inner layer 1 (Fig. 3b) is a ground plane with no segmentations, which helps reduce the impedance and the mutual inductance between circuits. This is very useful when working with digital systems. The ground plane was placed close to the top layer to reduce the path of return currents and reduce induced noises. The inner layer 2 (Fig. 3c) is the power plane. This plane was divided into three parts: a) the one that handles the supply voltage (V_{in}) coming from the USB port, b) the battery voltage V_{BAT}, and the supply voltage of the active circuits (V_{CC}). This prevents noise from the several power supplies from being scattered throughout the circuitry. Finally, the bottom layer (Fig. 3d) was used to trace some signal paths. However, this layer will be used to implement the microcontroller and wireless data transmission circuitry in the near future. Separating the analog and digital circuitry into different layers reduces crosstalk problems.

2.4 Power Supply and Data Acquisition System

All circuits were powered by a 3.7 V/250 mAh Lithium Polymer (LIPO) battery. The POKIT Pro (POKIT) system was used for data acquisition, which can be configured as a portable multimeter, oscilloscope, and data logger. To record the signals, the POKIT Pro was configured as an oscilloscope and acquired the signals at a sampling rate of 1 kSa/s. The signals were displayed on a mobile device with Android, and later the data was downloaded in .csv format.

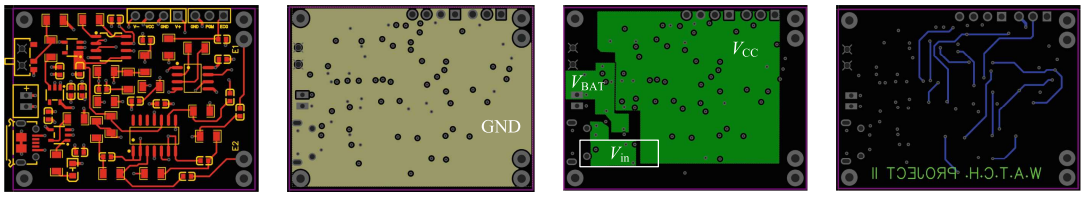

(a) (b) (c) (d)

Fig. 3. Design of the 4-layer PCB: a) Top layer, b) Inner layer 1 (Ground Plane), c) Inner layer 2 (Power Plane), and d) Bottom layer.

2.5 Volunteer

To be eligible for participation in the present study, subjects needed to be adults without diagnosed cardiac disease. Individuals of both genders could participate, while pregnant women and children were excluded. Following these criteria, one of the authors of the present work, who provided informed consent, was the test volunteer.

3 Results

The Z_{D} of the ECG circuit was 3.2 GΩ, and Z_{C} was 1.8 GΩ. Considering the contact impedance of the dry electrodes used, the loading error was lower than 0.002%. The total CMRR was about 80 dB, and the bandwidth was limited between 0.5 Hz and 40 Hz,

with a total gain of 60 dB, approximately. Regarding the cardiac pulse circuit, the total gain was about 50 dB, the CMRR was 70 dB, and the bandwidth was limited between 0.1 Hz and 10 Hz.

The PCB manufactured with all the implemented circuits is shown in Figs. 4a and 4b. The dimensions of the board allowed it to be incorporated into a custom-built case where two dry Ag-AgCl electrodes were also incorporated. In Figs. 4c and 4d, the device worn on the wrist of the volunteer is shown. To detect the ECG, the user must touch electrode 1 using a finger (e.g., index finger) of the hand that does not wear the device. Electrode 2 contacts the skin of the wrist that wears the device; in this way, lead-I is obtained. Figure 4d shows the TMR2001 sensor and the magnet placed on the radial artery, making it possible to detect the disturbance that causes the passage of blood to the localized magnetic field.

The overall consumption was less than 500 μA. Considering the battery capacity (250 mAh), the autonomy of this system measuring continuously (worst case) would be 500 h. However, this autonomy will be reduced by incorporating the microcontroller and the wireless data transmission system.

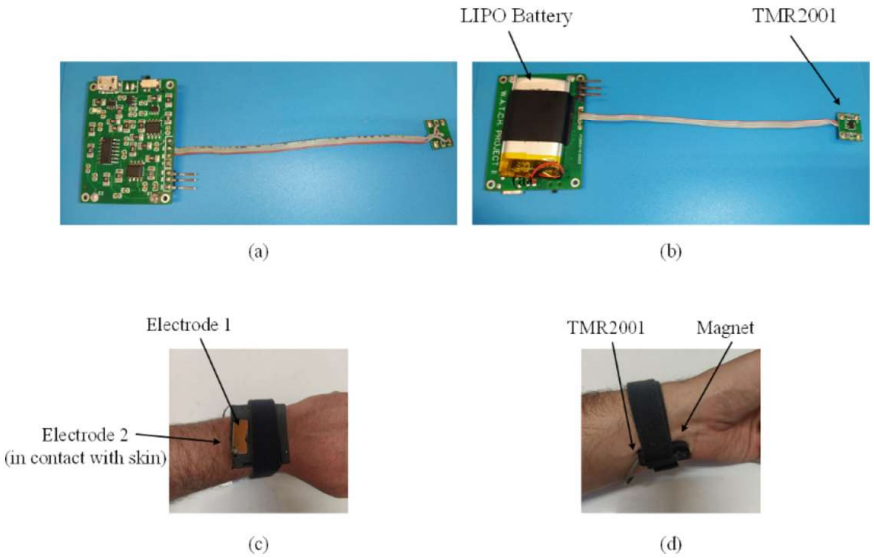

Fig. 4. a) Top layer of the PCB with all the electronic components assembled, b) Bottom layer of the PCB, the LIPO battery, and TMR2001 sensor, c) the custom-built case where de PCB was included, d) the TMR2001 sensor and the magnet placed near the radial artery.

Figure 5 shows the signals obtained with the developed device. The upper trace shows the result obtained with the patient simulator. All ECG waves are clearly depicted and without distortion. The middle trace shows the lead-I obtained from the volunteer, where a larger noise contribution is observed. This is due to electrode-skin contact because the skin was not prepared before the test. Even so, the SNR of the signal was higher than 68 dB, and the ECG waves could be distinguished, allowing the estimation of intervals and amplitudes of interest using simple signal processing algorithms. Considering the dimensions of the PCB ground plane, C_{ISO} was estimated according to [15]; in our case, $C_{ISO} \approx 1.4$ pF (Z_{ISO} @ 60Hz ≈ 1.9 GΩ). Assuming $\Delta Z_E = 5$ kΩ, $Z_C = 1.8$ GΩ, CMRR

= 80 dB, and using the values proposed in [16], that is: $C_B \approx 200$ pF (Z_B @ 60Hz $\approx$ 13 MΩ) and $i_p = 100$ nA, from (1), $V_{EMI} = 42.5$ μV when the device was used in an office, which implies a very low contribution from the power line interference. The lower trace displays the cardiac pulse signal obtained by measuring the magnetic disturbance of the blood. The signal had an SNR > 55 dB, where the systolic and diastolic amplitudes and the dicrotic notch are clearly shown.

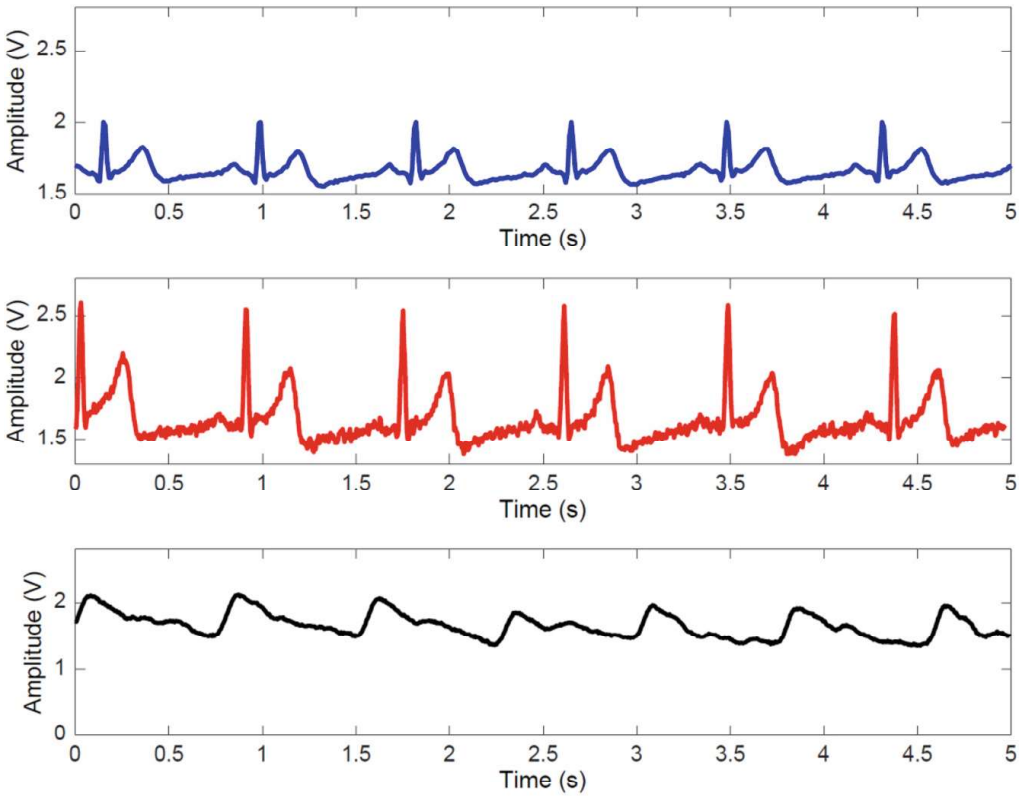

Fig. 5. Cardiac signals detected with the proposed device: From the patient simulator (upper trace), Lead-I ECG from a volunteer (middle trace), and cardiac pulse signal from a volunteer (bottom trace).

4 Conclusions

The preliminary design of a device capable of simultaneously detecting ECG and cardiac pulse was presented. The current consumption of the system was lower than 500 μA, and it was able to detect signals with an SNR greater than 55 dB. Thanks to the dimensions of the electronic circuitry, the interference contribution was lower than 42.5 μV. This suggests that the designed system can be implemented in a wearable device and is suitable for use in regular spaces where electromagnetic interferences are normally present. With this preliminary design, it is possible to develop a wearable system where simple signal processing algorithms can be implemented in such a way that it is possible to assess and track the cardiovascular health of a subject in non-hospital settings.

References

1. Skyrme, T., Dale, S.: IDTECH: Wearable Technology Forecasts 2023–2033. https://www.idtechex.com/en/research-report/wearable-technology-forecasts-2023-2033/928
2. Ates, C., Ates, H.C., Nguyen, P.Q., Gonzalez-Macia, L.: et al. End-to-end design of wearable sensors. Nat. Rev. Mater. **7**, 887–907 (2022). https://doi.org/10.1038/s41578-022-00460-x
3. Min, W., Wu, M., Luo, J.: Wearable technology applications in healthcare: a literature review. Online J. Nurs. Inform. **23**(3) (2019). https://www.himss.org/resources/wearable-technology-applications-healthcare-literature-review#_ENREF_30
4. Mannhart, D., et al.: Clinical validation of 5 direct-to-consumer wearable smart devices to detect atrial fibrillation: BASEL wearable study. clinical Electrophysiology **9**(2), 232–242 (2023)
5. Qermane, K., Mancha, R.: WHOOP Inc: digital entrepreneurship during the Covid-19 pandemic. Entrepreneurship Educ. Pedagogy **4**(3), 500–514 (2021)
6. Knecht, D.S., et al.: Technical characterization of the single-lead electrocardiogram signal from four different smartwatches and its clinical implications. Europace, **25**(Suppl 1) (2023)
7. Li, K., Elgalad, A., Cardoso, C., Perin, E.C.: Using the apple watch to record multiple-lead electrocardiograms in detecting myocardial infarction: where are we now? Tex. Heart Inst. J. **49**(4), e227845 (2022)
8. Spinelli, E.M., Mayosky, M.A.: Two-electrode biopotential measurements: power line interference analysis. IEEE Trans. Biomed. Eng. **52**(8), 1436–1442 (2005)
9. Ebrahimi, Z., Gosselin, B.: Ultra-low power photoplethysmography (PPG) sensors: a methodological review. IEEE Sens. J. (2023)
10. Pelaez, E.A., Villegas, E.R.: LED power reduction trade-offs for ambulatory pulse oximetry. In: 2007 29th Annual International Conference of the IEEE Engineering in Medicine and Biology Society, pp. 2296–2299. IEEE (2007)
11. Phua, C.T., Lissorgues, G., Mercier, B.: Non-invasive acquisition of blood pulse using magnetic disturbance technique. In: 13th International Conference on Biomedical Engineering: ICBME 2008 3–6 December 2008 Singapore, pp. 786–789. Springer Berlin Heidelberg (2009). https://doi.org/10.1007/978-3-540-92841-6_193
12. Méndez-Lira, O.A., Gutiérrez-Chávez, A., Cota-Ruiz, J.D., Díaz-Román, J.D., González-Landaeta, R.E.: Sistema Vestible para la Detección Simultánea y No Invasiva del ECG y el Flujo Sanguíneo. Revista mexicana de ingeniería biomédica **39**(3), 249–261 (2018)
13. Pallas-Areny, R., Colominas, J., Rosell, J.: An improved buffer for bioelectric signals. IEEE Trans. Biomed. Eng. **36**(4), 490–493 (1989)
14. Casas, O., Spinelli, E.M., Pallas-Areny, R.: Fully differential AC-coupling networks: a comparative study. IEEE Trans. Instrum. Meas. **58**(1), 94–98 (2008)
15. Catacora, V.A., Guerrero, F.N., Spinelli, E.M.: Size constraint to limit interference in drl-free single-ended biopotential measurements. J. Med. Biol. Eng. **42**(3), 332–340 (2022)
16. Haberman, M., Cassino, A., Spinelli, E.: Estimation of stray coupling capacitances in biopotential measurements. Med. Biol. Eng. Comput. **49**, 1067–1071 (2011)